

# Paul trapping of radioactive ${}^6\text{He}^+$ ions and direct observation of their $\beta$ -decay

X. Fléchar, <sup>1</sup> E. Liénard, <sup>1</sup> A. Méry, <sup>1,\*</sup> D. Rodríguez, <sup>1,†</sup> G. Ban, <sup>1</sup> D. Durand, <sup>1</sup> F. Duval, <sup>1</sup>  
M. Herbane, <sup>1,‡</sup> M. Labalme, <sup>1</sup> F. Mauger, <sup>1</sup> O. Naviliat-Cuncic, <sup>1</sup> J.C. Thomas, <sup>2</sup> and Ph. Velten <sup>1</sup>

<sup>1</sup>*LPC-Caen, ENSICAEN, Université de Caen, CNRS/IN2P3-ENSI, Caen, France*

<sup>2</sup>*GANIL, CEA/DSM-CNRS/IN2P3, Caen, France*

(Dated: November 9, 2018)

We demonstrate that abundant quantities of short-lived  $\beta$  unstable ions can be trapped in a novel transparent Paul trap and that their decay products can directly be detected in coincidence. Low energy  ${}^6\text{He}^+$  (807 ms half-life) ions were extracted from the SPIRAL source at GANIL, then decelerated, cooled and bunched by means of the buffer gas cooling technique. More than  $10^8$  ions have been stored over a measuring period of six days and about  $10^5$  decay coincidences between the beta particles and the  ${}^6\text{Li}^{++}$  recoiling ions have been recorded. The technique can be extended to other short-lived species, opening new possibilities for trap assisted decay experiments.

PACS numbers: 37.10.Rs; 37.10.Ty; 23.40.-s;

Atom and ion traps have found a wide range of applications in nuclear physics for the confinement of radioactive species [1, 2]. In particular, the continuous improvements in magneto-optical trapping efficiencies achieved since more than ten years [3, 4, 5, 6] resulted in a number of precision measurements for the study of fundamental interactions [7, 8, 9] as well as for the determination of nuclear static properties [10, 11]. The environment offered by traps in beta decay measurements is ideal to reduce instrumental effects, like the electron scattering in matter, or to enable the direct detection of recoiling ions. Such conditions led to measurements of angular correlation coefficients in beta decay with unprecedented precision [8, 9] motivated by the search for exotic interactions as signatures of physics beyond the standard electroweak model [12].

Although the principles for ion trapping [13, 14] were established well before those for the magneto-optical confinement [15], the consideration of ion traps for beta decay experiments with radioactive species is more recent. Technically, magneto-optical traps are often limited to alkali elements, for which suitable lasers can be found. They enable to produce samples of smaller size and with atoms at lower energies than ion traps. More elaborated transition schemes have recently been applied to radioactive He atoms [10, 11]. However, the efficiencies achieved so far with noble gas atoms in MOTs are too small for practicable precision measurements of beta decay correlations.

The standard geometry of a 3D-Paul trap [14], in which the hyperbolic electrodes are made of massive materials, is not well suited for the detection of decay products following beta decay. Ion confinement of radioactive species requires also the beam preparation for an efficient trapping [16] and such techniques posed new challenges when applied to light mass species.

In this paper we demonstrate that significant quantities of radioactive  ${}^6\text{He}^+$  ions can be confined in a novel Paul trap and that their decay products can directly be

detected, enabling thereby new trap assisted decay experiments. The results presented here were motivated by a new measurement of the  $\beta\bar{\nu}$  angular correlation coefficient in the Gamow-Teller decay of  ${}^6\text{He}$  to search for possible exotic interactions in nuclear beta decay. For this purpose, beta particles and recoiling ions are detected in coincidence to deduce the time of flight spectrum of ions relative to the beta particles.

The experiment has been carried out at the new low energy beam line LIRAT [17] of the SPIRAL facility at GANIL, firstly commissioned with radioactive beams in 2005. The  ${}^6\text{He}^+$  ions were produced from a primary  ${}^{13}\text{C}$  beam at 75 MeV/A impinging on a graphite target coupled to an ECR source. The source is located on a high voltage platform at 10 kV, what determines the kinetic energy of the extracted ions. The beam is then mass separated by a dipole magnet having a resolving power  $M/\Delta M \approx 250$ . After separation in  $m/q$ , the beam is composed of  ${}^6\text{He}^+$  and of stable  ${}^{12}\text{C}^{2+}$  ions. By adjusting the setting of the first magnet and the aperture of slits located after the magnet it was possible to significantly reduce the  ${}^{12}\text{C}^{2+}$  contribution at the expenses of a reduction in the  ${}^6\text{He}^+$  intensity by a factor of about 2. The resultant  ${}^{12}\text{C}^{2+}$  intensity does not affect the beam preparation before injection into the Paul trap.

The setup for the beam preparation (Fig. 1) is comprised of a radio frequency quadrupole cooler and buncher (RFQCB) followed by two pulsed electrodes located before the Paul trap. The beam intensity at the entrance of the RFQCB was typically 10 nA, including the contribution of the stable  ${}^{12}\text{C}^{2+}$  ions. Under optimal conditions, the  ${}^6\text{He}^+$  beam intensity was deduced to be  $2 \times 10^8 \text{ s}^{-1}$  by implanting a fraction of the beam into a Si detector.

The beam was cooled in the RFQCB using the buffer gas technique [16], which is relatively fast and universal, and well suited for radioactive species. Since the cooling is only efficient at energies of about 100 eV, the RFQCB is mounted on a high-voltage platform, operated 100 V

below the voltage of the ECR source platform. In the RFQCB, the ions are confined radially by an RF field applied to four cylindrical rods. The rods are segmented in order to generate a longitudinal electrostatic field which drives the ions toward the exit of the structure. A detailed description of the device can be found elsewhere [18]. The cooling of ions as light as  $^4\text{He}^+$  had previously been demonstrated using  $\text{H}_2$  as buffer gas [19]. Inside the cooler, the ions are accumulated to produce a bunch for an efficient injection in the Paul trap. The bunch is extracted from the RFQCB by fast switching the buncher electrodes after thermalization of ions with the buffer gas.

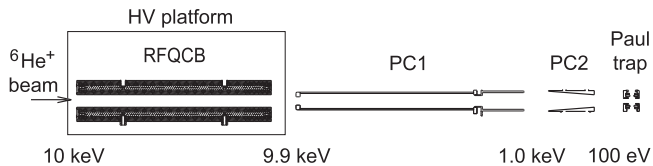


FIG. 1: Beam preparation scheme showing the RFQCB and two pulsed cavities located upstream from the Paul trap (distances between the elements are not to scale). The total mean energy of ions is indicated at different steps.

The ions are then transported through a first pulsed cavity (PC1) followed by an electrostatic lens (not shown on Fig. 1) and finally through a second pulsed cavity (PC2) before their injection into the Paul trap. Switching voltages applied to PC1 and PC2 reduce the mean ion energies from 9.9 keV to 1 keV and then from 1 keV to 100 eV respectively [20] in order to achieve an efficient capture of the ion bunch by the Paul trap.

The ion bunches are injected in the Paul trap at a repetition rate of 10 Hz. The electric field inside the trap is generated by two pairs of coaxial rings separated by 10 mm (Fig. 2), and is close to a quadrupole field over few  $\text{mm}^3$  around the trap center [20]. The frequency used in the trap was 1.15 MHz for a 130 V peak-to-peak voltage amplitude. The RF voltage is applied on the two inner rings whereas the outer rings are grounded. The RF signal on the trap was continuously applied during the measuring cycles. The overall performance of the system has been thoroughly tested with stable  $^4\text{He}^+$ ,  $^{35}\text{Cl}^+$  and  $^{36,40}\text{Ar}^+$  ions from the ECR source [20] and with  $^6\text{Li}^+$  ions from a surface ionization source [22]. Considering the duty cycle used for the injection of the  $^6\text{He}^+$  bunches into the trap, the beam preparation efficiency was estimated to be  $7 \times 10^{-5}$ , including the deceleration, cooling, bunching, transmissions through the pulsed cavities and trapping.

The trap geometry allows the application of suitable voltages on the rings for the injection and extraction of ions. The absence of a massive ring electrode also enables the direct detection of products from decays in the trap. The trap is surrounded by an electron telescope detector and by two ion detectors (Fig. 2). Collimators located in

front of the detectors enable the selection of events originated mainly in the trap. The number of trapped ions was continuously monitored by counting the ions remaining in the trap after a fixed storage time, using the micro-channel plate (MCP) detector located downstream. This detector is preceded by three grids to reduce the intensity of the incident ion bunches. The measured time-of-flight distribution contains a single peak corresponding to a mass-to-charge ratio  $Q/A = 6$ . The storage time of ions in the trap, deduced from the rate of coincidence events and accounting for the  $\beta$ -decay, was 240 ms for a typical pressure in the trap chamber of  $2 \times 10^{-6}$  mbar due to  $\text{H}_2$  gas leaking from the RFQCB. The main effect limiting the storage time of ions inside the trap is the collision of ions with molecules of the residual gas.

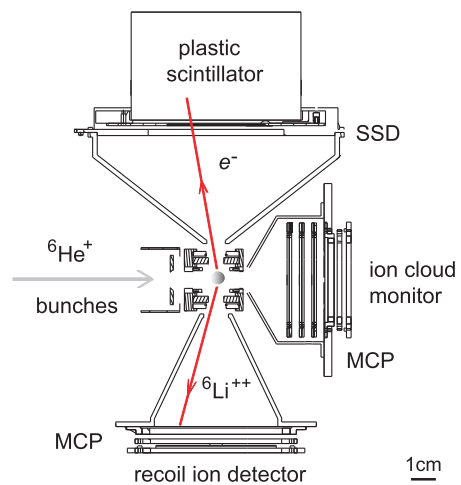


FIG. 2: Experimental setup with the transparent Paul trap surrounded by the beta particle telescope and the two ion detectors. The scale indicates the size of this table top experiment.

The telescope for beta particles is composed of a  $60 \times 60 \text{ mm}^2$ ,  $300 \mu\text{m}$  thick, double-sided position sensitive silicon strip detector (SSD), with  $2 \times 60$  strips for horizontal and vertical location. The SSD is followed by a  $\text{Ø}11 \times 7 \text{ cm}^2$  plastic scintillator. To achieve a better vacuum in the trap chamber, both detectors are located in an evacuated chamber separated from the trap chamber by a  $1.5 \mu\text{m}$  thick mylar foil. The recoil ion detector uses two MCPs with delay-line readout providing position sensitivity. The time resolution of the detector is smaller than 200 ps. The dependence of the detector efficiency as a function of the ion kinetic energy, the incidence angle and the position has been studied in detail and was described elsewhere [21]. An acceleration voltage is applied on an electrode located 6 mm in front of the MCP. The ion detection efficiency reaches 53% for post-accelerating voltages larger than 4 kV.

The trigger of an event is generated by a signal in the

plastic scintillator. The 120 strips of the SSD are then read-out sequentially by multiplexing the signals. The trigger also generates the start signal for the time measurement relative to the MCP detector located opposite to the trap. Under regular conditions, the average trigger rate was  $200 \text{ s}^{-1}$ . Most of these events were singles, for which only the signal of the energy deposited in the plastic scintillator was recorded along with the position and energy information from the 120 strips of the SSD. For coincidence events, six other parameters were additionally stored: *i*) the time difference between the plastic scintillator and the MCP signal; *ii*) the charge in the MCP; and *iii-vi*) the time differences between the signal from the MCP and the four outputs of the delay lines (two for each coordinate) for the position reconstruction. For all events, the time within the cycle relative to the extraction pulse from the RFQCB as well as the RF phase in the Paul trap were also recorded for later study of the ion cloud stability and control of instrumental effects.

With the position information of the beta particle and of the recoiling ion, it is possible to reconstruct the rest mass of the anti-neutrino from the decay kinematics which provides a useful control means to identify background sources. The spectrum built after energy calibration of the plastic scintillator and selection of beta particles with energies above 1 MeV is shown in Fig. 3. Two other conditions were imposed to the data: 1) the signal in the SSD should have a valid conversion in the vertical and horizontal positions, corresponding to a minimum ionizing particle; 2) the coincidence must be recorded at least 20 ms after the injection of the ion bunch in the trap, which is needed for the ions to reach the thermal equilibrium.

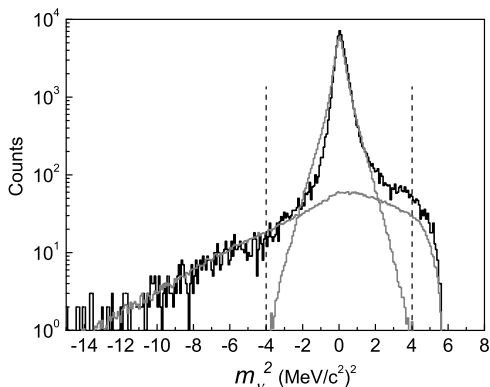


FIG. 3: Anti-neutrino rest mass spectrum reconstructed from the decay kinematics (black) and compared with results from MC simulations (gray). The main peak corresponds to decay events occurring in the trap. The broad asymmetric distribution is due to decays from neutral  ${}^6\text{He}$  atoms occurring outside of the trap and to accidental events. See text for details.

The measured spectrum is compared to a Monte-Carlo (MC) simulation which includes the geometry of the

setup, the size and temperature of the ion cloud inside the trap, the effect of the trap RF field on the ions inside the trap and during their recoil, and the energy resolution of the plastic scintillator. The simulation does however not include: the scattering of electrons on the matter surrounding the trap with the possible generation of secondary background, the response function of the plastic scintillator, the effect of ionization during  $\beta$ -decay [23] and other recoil order effects beyond the allowed approximation for the description of the beta decay process. For the purpose of this comparison, the value of the  $\beta\bar{\nu}$  angular correlation coefficient was assumed to be the one expected from the standard model for a pure Gamow-Teller transition,  $a_{GT} = -1/3$  [24]. The width of the signal peak in Fig. 3 is dominated by the phase space of ions inside the trap [22]. The two main background sources which have been identified, and which give both rise to asymmetric distributions in the anti-neutrino rest mass, are accidental coincidences and decay events of neutral  ${}^6\text{He}$  atoms produced in the RFQCB which diffuse into the trap chamber. Although the simplified MC simulation does not reproduce all details of the measured spectra, the discrepancies are not crucial to illustrate two main points: i) that the signal to background ratio in the region of the peak is about 100:1 and ii) that the largest fraction of the background is well identified as associated with decays out of the trap such that the setup can be improved for future precision measurements.

Figure 4 shows the time of flight spectrum of ions relative to the beta particle when selecting events with the condition  $\pm 4 \text{ (MeV}/c^2)^2$  on the anti-neutrino rest mass (Fig. 3). The data correspond to a total measuring time of about 6 days. Since the overall detection efficiency of the system is  $1.5 \times 10^{-3}$  [22], one concludes that more than  $10^8$  radioactive ions have been trapped during the measurement.

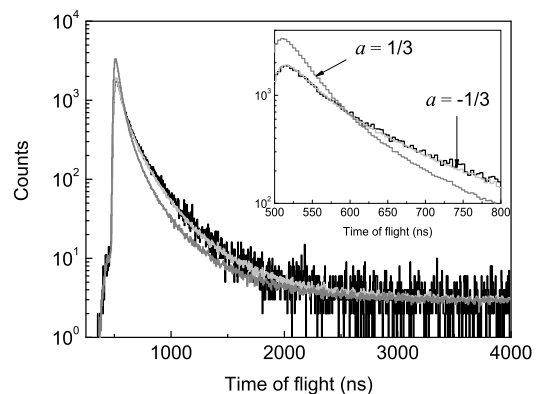


FIG. 4: Comparison between the experimental time-of-flight spectrum (black) and calculations from MC simulations, assuming either  $a = -1/3$  (light gray) or  $a = 1/3$  (dark gray). The insert shows the most sensitive interval to the value of the  $\beta\bar{\nu}$  angular correlation coefficient  $a$ .

The data in the time-of-flight spectrum has also been compared to the MC simulation. The edge of the spectrum, between 460 and 510 ns, which is weakly sensitive to the dynamics of the decay, served here to accurately determine the average distance between the ion cloud center and the recoiling ion detector, and is then not considered in the comparison. The value of the angular correlation coefficient was here fixed to either  $a_A = a_{GT} = -1/3$ , corresponding to pure axial couplings (light gray line in Fig.4), or to  $a_T = 1/3$  for pure tensor couplings (dark gray line in Fig.4). Since the number of events in the MC simulation is normalized to the number of measured events, there are then no free parameters in the comparison between the data and the MC. The fairly good agreement between the data and the MC for  $a_A = a_{GT}$  proves that the main features of the setup are well understood. The most sensitive interval of the spectrum to the angular correlation coefficient is located between 500 and 800 ns (see insert in Fig.4), where the signal-to-accidental ratio is 55. With the data presented here it is possible to determine the angular correlation coefficient with a statistical precision  $\Delta a/a = 0.018$ , what is a factor of 5 more precise than the most precise measurement of this coefficient from a coincidence measurement in  ${}^6\text{He}$  decay [25], showing the potential of this trapping technique.

The experiment presented above demonstrates that abundant quantities of radioactive ions can be efficiently trapped using a novel transparent Paul trap, and that their decay products can be recorded with suitable detectors. The technique has been tested with  ${}^6\text{He}^+$  ions, which are the lightest short-lived radioactive ions ever trapped. This required the extension of the buffer gas cooling technique to the lightest accessible masses [19] and its application to radioactive species. The trapping scheme provides significantly larger efficiencies for noble gas elements than those obtained so far with MOTs and offers a more suitable environment than Penning traps for the detection of decay products. The technique can be extended to any radioactive ion, such as for example  ${}^8\text{Li}^+$  or  ${}^{19}\text{Ne}^+$ , opening the possibility for new trap assisted decay experiments.

Since the completion of the experiment presented here, the efficiency of the beam preparation system was improved by almost two orders of magnitude [26] enabling the possibility for a high precision measurement of the angular correlation coefficient in  ${}^6\text{He}$  decay.

We are grateful to J. Bregeault, Ph. Desrues, B. Jacquot, Y. Merrer, Ph. Vallerand, Ch. Vandamme and F. Varenne for their assistance during the different phases of the project. We thank J. Blicke and Y. Lemièrre for their cooperation during the experiment. This work was supported in part by the Région Basse Normandie, by the NIPNET RTD network within the 6th FP (contract Nr HPRI-CT-2001-50034) and by the TRAPSPEC JRA within the I3-EURONS (contract Nr

506065). D. Rodríguez acknowledges support from the E.U. under a Marie Curie Intra-European Fellowship (contract Nr MEIF-CT-2005-011269).

- 
- \* Present address: SUBATECH, Ecole des Mines de Nantes, 44307 Nantes, France.
  - † Present address: Dep. de Física Aplicada, Univ. de Huelva, 21071 Huelva, Spain.
  - ‡ Present address: Dep. of Physics, College of Science, King Khalid Univ., Abha-Saudi Arabia.
- [1] G.D. Sprouse and L.A. Orozco, *Ann. Rev. Nucl. Part. Sci.* **47**, 429 (1997).
  - [2] G. Bollen, *Eur. Phys. J. A* **15**, 237 (2002) and references therein.
  - [3] Z.-T. Lu *et al.*, *Phys. Rev. Lett.* **72**, 3791 (1994).
  - [4] G. Gwinner *et al.*, *Phys. Rev. Lett.* **72**, 3795 (1994).
  - [5] J.A. Behr *et al.*, *Phys. Rev. Lett.* **79**, 375 (1997).
  - [6] R. Guckert *et al.*, *Phys. Rev. A* **58**, R1637 (1998).
  - [7] S.G. Crane *et al.*, *Phys. Rev. Lett.* **86**, 2967 (2001).
  - [8] N.D. Scielzo, S.J. Freedman, B.K. Fujikawa, and P.A. Vetter, *Phys. Rev. Lett.* **93**, 102501 (2004); P.A. Vetter, J.R. Abo-Shaeer, S.J. Freedman, and R. Maruyama, *Phys. Rev. C* **77**, 035502 (2008).
  - [9] A. Gorelov *et al.*, *Phys. Rev. Lett.* **94**, 142501 (2005).
  - [10] L.-B. Wang *et al.*, *Phys. Rev. Lett.* **93**, 142501 (2004).
  - [11] P. Mueller *et al.*, *Phys. Rev. Lett.* **99**, 252501 (2007).
  - [12] N. Severijns, M. Beck and O. Naviliat-Cuncic, *Rev. Mod. Phys.* **78**, 991 (2006).
  - [13] L. S. Brown and G. Gabrielse, *Rev. Mod. Phys.* **58**, 233 (1986), and references therein.
  - [14] W. Paul, *Rev. Mod. Phys.* **62**, 531 (1990), and references therein.
  - [15] W.D. Phillips and H. Metcalf, *Phys. Rev. Lett.* **48**, 596 (1982); E.L. Raab, M. Prentiss, A. Cable, S. Chu, and D.E. Pritchard, *Phys. Rev. Lett.* **59**, 2631 (1987).
  - [16] M.D. Lunney and R.B. Moore, *Int. J. Mass Spectrom.* **190/191**, 153 (1999).
  - [17] F. Varenne, *LIRAT: A very low energy beam line for radioactive ions*, in Technical Report on Operating Accelerators 2003-2004, internal report GANIL R-05-01, 2005.
  - [18] G. Darius *et al.*, *Rev. Sci. Instrum.* **75**, 4804 (2004).
  - [19] G. Ban *et al.*, *Nucl. Instrum. Meth. Phys. Res. A* **518**, 712 (2004).
  - [20] D. Rodríguez *et al.*, *Nucl. Instrum. Meth. Phys. Res. A* **565**, 876 (2006).
  - [21] E. Liénard *et al.*, *Nucl. Instrum. Meth. Phys. Res. A* **551**, 375 (2005).
  - [22] A. Méry, Ph.D. thesis, Université de Caen Basse-Normandie, 2007 (unpublished).
  - [23] The probability for the electron ionization, resulting in the  ${}^6\text{Li}^{3+}$  ion during beta decay, was calculated to be  $(233.8 + 0.4E_R) \times 10^{-4}$  as a function of the recoiling ion kinetic energy,  $E_R$  (in keV); Z. Patyk, private communication.
  - [24] J.D. Jackson, S.B. Treiman and H.W. Wyld, Jr., *Nucl. Phys.* **4**, 206 (1957).
  - [25] J.B. Vise and B.M. Rustand, *Phys. Rev.* **132**, 2573 (1963).
  - [26] F. Duval *et al.*, *Nucl. Instrum. Meth. Phys. Res. B.*; 10.1016/j.nimb.2008.05.078